Copyright © 2009 by the Genetics Society of America
DOI: 10.1534/genetics.108.096008

Cell Survival and Polarity of Drosophila Follicle Cells Require the Activity of Ecdysone Receptor B1 Isoform

Patrizia Romani,* Fabio Bernardi,* Jennifer Hackney,† Leonard Dobens,† Giuseppe Gargiulo* and Valeria Cavaliere*,[1]

**Dipartimento di Biologia Evoluzionistica Sperimentale, Università di Bologna, Bologna, Italy, 40126 and †Division of Molecular Biology and Biochemistry, School of Biological Sciences, University of Missouri, Kansas City, Missouri 64110*

Manuscript received September 10, 2008
Accepted for publication November 11, 2008

ABSTRACT

Proper assembly and maintenance of epithelia are critical for normal development and homeostasis. Here, using the Drosophila ovary as a model, we identify a role for the B1 isoform of the ecdysone receptor (EcR-B1) in this process. We performed a reverse genetic analysis of EcR-B1 function during oogenesis and demonstrate that silencing of this receptor isoform causes loss of integrity and multilayering of the follicular epithelium. We show that multilayered follicle cells lack proper cell polarity with altered distribution of apical and basolateral cell polarity markers including atypical-protein kinase C (aPKC), Discs-large (Dlg), and Scribble (Scrib) and aberrant accumulation of adherens junctions and F-actin cytoskeleton. We find that the EcR-B1 isoform is required for proper follicle cell polarity both during early stages of oogenesis, when follicle cells undergo the mitotic cell cycle, and at midoogenesis when these cells stop dividing and undergo several endocycles. In addition, we show that the EcR-B1 isoform is required during early oogenesis for follicle cell survival and that disruption of its function causes apoptotic cell death induced by caspase.

MAINTENANCE of epithelial cell architecture is crucial to normal tissue function and defects in this process can cause organ dysplasia and systemic diseases. Epithelial cells are polarized and in most cases this polarity is required for functionality of an epithelium. Junctions connecting epithelial cells define distinct apical and basolateral membrane domains. The core molecular mechanisms underlying epithelial polarization are evolutionarily conserved across animal species (Tepass *et al.* 2001). In Drosophila, three protein complexes have been identified that specify apical and basolateral membrane domains (Müller and Bossinger 2003). The Bazooka (Baz) complex (Baz/aPKC/Par6) specifies the apical domain. The apicalizing activity of the Baz complex is repressed by the Scribble complex (Scrib/Dlg) that acts as a basolateral determinant. The Crumbs (Crb) complex (Crb/Stardust/DPATJ) localizes to the apical membrane to antagonize the Scrib complex.

Although efforts have been made to elucidate the mechanisms that specify cell polarity, there are still many open questions about how this cell architecture is established and maintained. The identification of signaling pathways controlling epithelial morphogenesis should further our understanding of this complex process. The follicular epithelium surrounding the Drosophila egg chamber represents a well-characterized and genetically tractable model for addressing these studies. Oogenesis starts within the germarium where new egg chambers are generated from an interaction between somatic and germline stem cells. Egg chamber development proceeds within a shared ovariole according to a program of continuous growth and differentiation, which is divided into 14 stages (Spradling 1993; Wu *et al.* 2008). At the beginning of oogenesis when the stage 1 egg chamber leaves the germarium, the somatic follicle cells form a monolayer that surrounds each 16-cell germline cyst. The follicular epithelium is polarized with the apical side facing the germline and the basal side facing the epithelial sheath surrounding each string of developing egg chambers. Follicle cells surrounding the egg chamber undergo mitotic divisions to keep pace with germline cell growth. By stage 7, the follicle cells cease divisions and undergo three rounds of endoreplication. After stage 6, follicle cells begin to show morphological and molecular signs of differentiation into the five main epithelial fates: border, stretched, centripetal, posterior, and main body follicle cells.

Programmed cell death (PCD) plays a central role in animal development eliminating unwanted tissue, controlling cell numbers, and removing cells that are dangerous for the organisms. PCD during Drosophila oogenesis occurs at distinct stages and is triggered by both developmental and environmental stimuli (McCall 2004). Proper development of every oocyte requires develop-

[1]*Corresponding author:* Dipartimento di Biologia Evoluzionistica Sperimentale, Via Selmi 3, 40126, Bologna, Italy.
E-mail: valeria.cavaliere@unibo.it

mentally regulated apoptotic-like death of nurse cells. Starting from stage 10B a massive cytoplasmic dumping of nurse cell contents into the oocyte occurs and from stage 12 DNA fragmentation and nuclear condensation follow. Poor environmental conditions can also induce stage-specific PCD during oogenesis (McCall 2004). Degeneration of egg chambers in region 2A of the germarium frequently occurs in females subjected to nutrient deprivation. Limited nutrients or other insults can also induce PCD as a physiological response in nurse cells of midstage egg chambers leading to entire egg chamber degeneration.

Final effectors of PCD are caspases, a highly specialized class of cysteine proteases, whose activation is tightly controlled and occurs through proteolytic processing (Danial and Korsmeyer 2004). Caspases are negatively regulated by inhibitor of apoptosis proteins (IAPs) a highly conserved class of proteins that directly binds and inhibits caspases (Steller 2008). Differing from developmental nurse cell PCD that only partially requires caspase activity, midstage PCD is caspase dependent (Peterson *et al.* 2003; Baum *et al.* 2007).

A critical balance between death activators and death inhibitors determines the decision to live or to die. The steroid hormone ecdysone is one of the signals that could affect this balance regulating the patterns of PCD in a precise temporal and spatial pattern (Yin and Thummel 2005). Ecdysone is responsible for coordination of embryogenesis, larval molting, and metamorphosis and it plays multiple regulatory roles in coordinating the formation of a mature egg (Bownes 1989). Ecdysone signaling regulates the key checkpoint in egg chamber maturation at stages 8–9 of oogenesis (Terashima and Bownes 2004, 2005) and it is believed that it is also involved in the germarium checkpoint (McCall 2004). Recently, it has been reported that ecdysone and Ras signaling modulate follicle cell differentiation and cell-shape changes (Hackney *et al.* 2007). Ecdysone signaling in Drosophila is controlled by a heteromeric receptor composed of the ecdysone receptor (EcR) and ultraspiracle (USP) (Riddiford *et al.* 2000). Three EcR isoforms—EcR-A, EcR-B1, and EcR-B2—share a common C-terminal region that contains DNA-binding and ligand-binding domains but differ at their N-terminal domain (Talbot *et al.* 1993). As well, EcR isoforms exhibit different spatial and temporal expression patterns and induce different cellular responses (Talbot *et al.* 1993).

In this study, we investigate the involvement of the ecdysone signaling pathway in follicular epithelial maintenance and cell survival. We use reverse genetic approaches to knock down EcR-B1 function in follicle cells to show that EcR-B1 is required for proper follicular epithelium polarity and maintenance. In addition we find that silencing of EcR-B1 in follicle cells at early stages of oogenesis causes apoptotic cell death accomplished through Diap1 downregulation and caspase activation.

MATERIALS AND METHODS

Fly strains: Stocks were raised on standard cornmeal/yeast/agar medium at 25°, and crosses were carried out at the same temperature unless otherwise stated. yw^{67c23} was used as the wild-type stock in this study. We used the following stocks: (1) *UAS-EcR.B1.dsRNA* stock (Bloomington Stock Center stock 9329; genotype w^{1118}*; +; P{w*$^{+mC}$*=UAS-EcR.B1.dsRNA}168*); (2) *P{ry*$^{+}$*, hsFLP}, y*^{1}*, w*^{1118}*; Dr*^{Mio}*/TM3, ry, Sb*^{1} (Bloomington stock 7); (3) *y*^{1}*, w* P{w*$^{+mC}$*=GAL4-Act5C(FRT.CD2).P}D* (Bloomington stock 4779); (4) *Cy2-Gal4* (Queenan *et al.* 1997) (genotype *w*; Cy2-Gal4; P{w*$^{+mC}$*=tubP-GAL80*^{ts}*}7*) (kindly provided by T. Schüpbach, Princeton University); and (5) *E4-Gal4* (Queenan *et al.* 1997) (genotype *w*; +; E4-Gal4*) (kindly provided by T. Schüpbach, Princeton University). The *w*; P{w*$^{+mC}$*=tubP-GAL80*^{ts}*}20; TM6B/P{w*$^{+mC}$*=tubP-GAL4}LL7* was generated in Gargiulo's lab starting from *y*^{1}*, w*; +; P{w*$^{+mC}$*=tubP-GAL4}LL7/TM3, Sb*^{1} (Bloomington stock 5138) and *w*; P{w*$^{+mC}$*=tubP-GAL80*^{ts}*}20; TM2/TM6B, Tb*^{1} (Bloomington stock 7019).

Clonal analyses: Clonal overexpression of *UAS-EcR.B1.dsRNA* transgene was obtained using the Flp-out/Gal4 technique (Pignoni and Zipursky 1997) by crossing the appropriate fly strains. Freshly eclosed females of the genotype *P{ry*$^{+}$*, hsFLP}, y*^{1}*, w*^{1118}*/y*^{1}*, w, P{w*$^{+mC}$*=GAL4-Act5C(FRT.CD2).P}D; +; P{w*$^{+mC}$*=UAS-EcR.B1.dsRNA}168* were collected and heat shocked four times for 1 hr at 37°. After each heat shock these females were transferred to fresh vials with yw^{67c23} males and incubated at 25°. Before dissection, the flies were transferred to fresh, yeasted food daily at 29° for 7 days.

Gal4 driven expression in follicle cells: Females *w*; Cy2-Gal4/+; P{w*$^{+mC}$*=tubP-GAL80*^{ts}*}7/P{w*$^{+mC}$*=UAS-EcR.B1.dsRNA}168* and *w*; +; E4-Gal4/P{w*$^{+mC}$*=UAS-EcR.B1.dsRNA}168* were obtained by crossing the parental strains. The crosses were performed at 18°. The progeny was transferred with yw^{67c23} males to yeasted vials at 18° for 48 hr and then to yeasted vials at 31° for 24 hr before dissection. Females *w*; P{w*$^{+mC}$*=tubP-GAL80*^{ts}*}7/+; P{w*$^{+mC}$*=UAS-EcR.B1.dsRNA}168/ P{w*$^{+mC}$*=tubP-GAL4}LL7* were obtained by crossing the parental strains. The crosses were performed at 18° and before dissection, the progeny were transferred with yw^{67c23} males to yeasted vials at 31° for 6 days.

Immunofluorescence microscopy: Fixation and antibody staining of hand-dissected ovaries were carried out as previously described (Andrenacci *et al.* 2001). Monoclonal anti-EcR-B1 1:10 (AD4.4, DSHB), anti-Arm 1:10 (N2A 71, DHSB), anti-CD2 1:250 (MCA154G, Serotec), anti-DE-Cad 1:25 (DCAD2, DSHB), anti-Dlg 1:50 (4F3, DSHB), and anti-Diap1 1:100 (a gift from B. Hay) antibodies were used and detected with TEXAS-RED-conjugated anti-mouse secondary antibody (1:400, Invitrogen), Cy5-conjugated anti-mouse secondary antibody (1:200, Jackson), or FITC-conjugated anti-mouse secondary antibody (1:250, Invitrogen). Rabbit anti-phosphohistone H3 (Upstate Biotechnology), anti-Scrib (a gift from C. Doe), and anti-aPKC (Santa Cruz Biotechnology) were used at 1:200 dilution while anti-cleaved caspase-3 (Cell Signaling Technology) was used at 1:50 dilution. Rabbit antibodies were detected with Cy3-conjugated anti-rabbit secondary antibody (1:1000, Sigma), Cy5-conjugated anti-rabbit secondary antibody (1:200, Jackson), or BODIPY-conjugated anti-rabbit secondary antibody (1:2000, Molecular Probes), respectively. DAPI staining was carried out by incubating the egg chambers for 10 min with DAPI (4′-6-diamidino-2-phenylindole, Sigma) at 1 μg/ml in PBS and, after several washes with PBS, the egg chambers were mounted. For propidium iodide nuclear counterstaining the ovaries were washed three times in PBT and treated with RNase A (400 μg/ml in PBS, Sigma) for 2 hr. After three 10-min washes in PBT, the ovaries were labeled for

15 min with propidium iodide (5 μg/ml in PBT, Molecular Probes). Afterward, the egg chambers were washed three times in PBT. FITC-phalloidin staining was carried out by incubating the egg chambers for 20 min at room temperature with FITC-phalloidin (40 μg/ml in PBS, Sigma), and after several washes with PBT, the egg chambers were mounted. Stained egg chambers were mounted in Fluoromount-G (Electron Microscopy Sciences) for DAPI and propidium iodide nuclear staining and were subsequently analyzed with conventional epifluorescence on a Nikon Eclipse 90i microscope and with TCS SL Leica confocal system.

Terminal deoxynucleotidyl transferase-mediated dUTP nick end labeling: Isolated ovaries were fixed as previously described (Cavaliere *et al.* 1998). Terminal deoxynucleotidyl transferase-mediated dUTP nick end labeling (TUNEL) and DAPI stainings were carried out substantially as described (Cavaliere *et al.* 1998) except that digoxigenin-conjugated dUTP was revealed by using anti-digoxigenin-fluorescein conjugated antibody (1:100, Roche). After three washes in PBS they were incubated, with agitation, for 30 min in 0.1% Triton X-100, 0.1% sodium citrate. The ovaries were washed twice with PBS and treated for 90 min at 37°, with agitation, with 10 μM digoxigenin-11-dUTP, 0.2 units/μl of terminal transferase, 1× terminal transferase buffer (Roche), and 2.5 mM $CoCl_2$. After five washes with PBT and one wash in 3% BSA in PBT, the ovaries were treated for 60 min, with agitation, with anti-digoxigenin-fluorescein conjugated antibody. The ovaries were extensively washed with PBT and stained for 10 min with DAPI 1 μg/ml in PBS. After several washes with PBS, the egg chambers were mounted in Fluoromount-G and examined by epifluorescence under a Nikon Eclipse 90i microscope.

RESULTS

Ubiquitous *EcR-B1* silencing in the follicular epithelium strongly affects egg chamber development: The *EcR* locus, at 42A (Koelle *et al.* 1991), is proximal to available FRT insertion sites, preventing Flp-mediated mosaic analysis. Therefore we used a transgenic RNA interference approach coupled with the *UAS/Gal4* system (Brand and Perrimon 1993) to obtain *EcR-B1* knockdown in follicle cells (Kennerdell and Carthew 2000). We took advantage of the *UAS-IR-EcR-B1* transgene containing inverted repeat (IR) sequences designed to target the 5′ *EcR-B1*-specific exon β2 (Roignant *et al.* 2003). To test the effects of knocking down EcR-B1 levels, the transgene was expressed using the ubiquitous and strong *tub-Gal4* driver. To circumvent the associated lethality, we utilized the *tub-Gal80^{ts}* transgene encoding a temperature-sensitive form of the Gal4 inhibitor Gal80 (Gal80^{ts}), which blocks Gal4 activity at the permissive low temperature (18°), while it fails to inhibit Gal4 at the higher restrictive temperature (31°) (McGuire *et al.* 2003).

Previous genetic studies of mutations affecting all EcR protein products showed that EcR receptor controls multiple aspects of oogenesis and that it is also required for egg chamber integrity (Carney and Bender 2000). As shown in Figure 1, ubiquitous knockdown of EcR-B1 caused breakdown of egg chambers that is not detected in wild-type ovariole (Figure 1G). In 54% of mutant ovarioles ($n = 177$) we observed remnant egg chamber material as shown by FITC-phalloidin (Figure 1, A and D) and propidium iodide stainings (Figure 1, B and E). These results show that targeting *EcR-B1* RNAi in the follicular epithelium results in a phenotype similar to temperature sensitive *EcR* mutants, suggesting that this isoform plays a key role in maintenance of egg chamber integrity.

During midoogenesis EcR-B1 is required to maintain follicle cell polarity: To further analyze EcR-B1 function we carried out tissue- and stage-specific RNAi mediated knockdown of *EcR-B1* gene function using the *UAS/Gal4* system. We used the *Cy2-Gal4* driver, which promotes *UAS*-linked gene expression mainly in the follicle cells covering the oocyte from stage 7 onward (Queenan *et al.* 1997) (Figure 2A). Again, the *tub-Gal80^{ts}* system (McGuire *et al.* 2003) was employed in combination with this driver to avoid any lethal effects associated with *UAS-IR-EcR-B1* expression during development. As shown in Figure 2B, propidium iodide staining of follicle cell nuclei reveals the loss of monolayer integrity of the follicular epithelium during midoogenesis in these *Cy2-Gal4; UAS-IR-EcR-B1* egg chambers. The follicle cells accumulated in multiple layers and their nuclei have an altered shape and a high degree of DNA staining (dotted line in Figure 2B; dotted areas in Figure 2, D, G, and J). Piling up of follicle cells is variable (see arrows in Figure 2B) reflecting spotted and patchy *Cy2-Gal4* driver expression pattern (Figure 2A).

To assess if expression of the targeted interfering RNA was effective at reducing EcR-B1 protein levels, egg chambers from the same *Cy2-Gal4*; *UAS-IR-EcR-B1* females were immunostained with anti-EcR-B1 antibody (AD4.4). This antibody has been shown to detect EcR-B1 protein expressed in both germline and somatic follicle cells throughout oogenesis (Carney and Bender 2000). Delamination of follicle cells always occurs in follicular epithelium areas of strongly reduced EcR-B1 expression. As shown in Figure 2, C–K, follicle cells that show the multilayered phenotype localized at anterior (Figure 2D), lateral (Figure 2G), and posterior (Figure 2J) domains of the follicular epithelium exhibit quite undetectable EcR-B1 levels (Figure 2, C and E, F and H, I and K, respectively) indicating that delamination is associated with effective knockdown of EcR-B1 levels.

We next analyzed whether the multilayered epithelium was a result of late-stage overproliferation by immunodetection of the phospho-histone H3 (PH3) mitotic marker. In wild-type follicle cells, at stage 6 of oogenesis, Notch-Delta signaling induces the transition from mitotic cell cycle to endocycle so that after this stage the PH3 mitotic marker is not detected (Deng *et al.* 2001). We observed that after stage 6 the PH3 marker is never detected in *Cy2-Gal4; UAS-IR-EcR-B1* egg chambers, indicating that the multilayered epithelium does not arise from loss of proliferation control (data not shown).

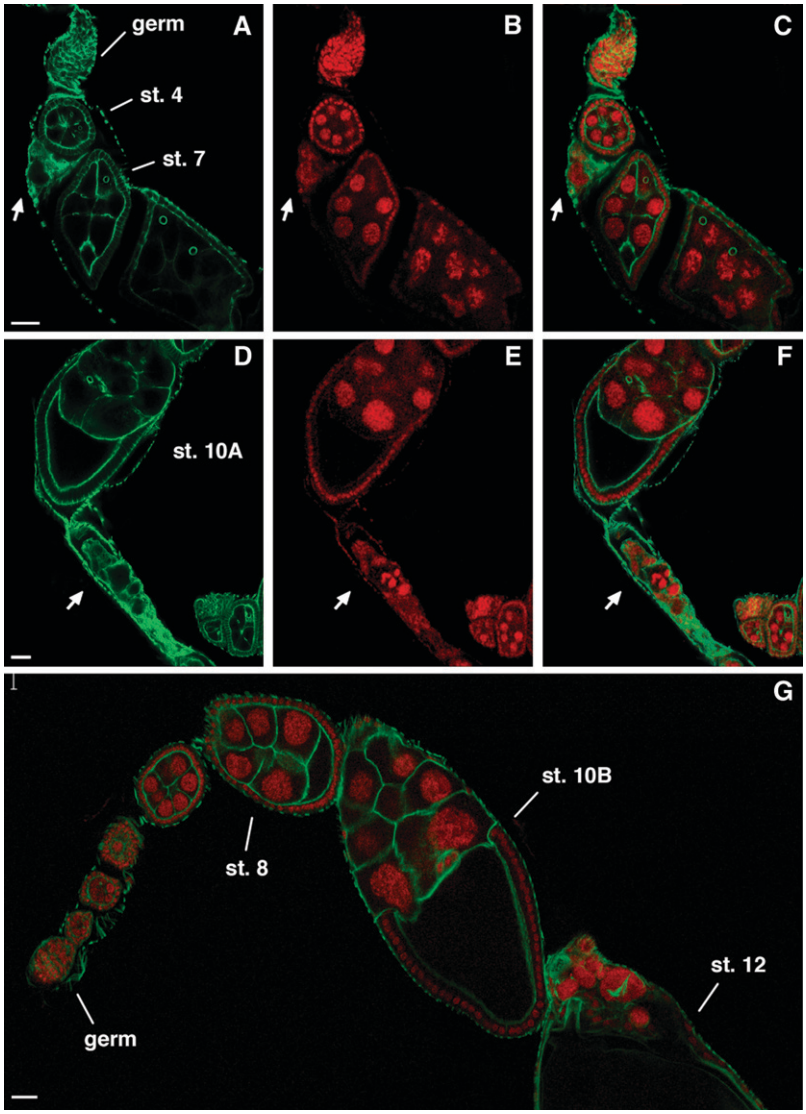

FIGURE 1.—Ubiquitous silencing of *EcR-B1* in the follicular epithelium induces egg chamber degeneration. Confocal cross-sections of ovarioles from females overexpressing the *UAS-IR-EcR-B1* transgene under the control of the *tub-Gal4* promoter (A–F) and from wild-type females (G). FITC-phalloidin (A and D; green), propidium iodide staining (B and E; red), and their merged signals (C and F) show the presence of degenerated egg chambers inside ovarioles (see white arrows). In comparison, in the wild-type ovariole (G) FITC-phalloidin and propidium iodide merged signals illustrate the absence of degenerating egg chambers. Anterior is up in all panels. Germ, germarium; st, stage. Bars, 20 μm.

Delamination of cells in multiple layers is a typical terminal phenotype for polarity defects in epithelial cells. Adherens junctions (AJs), considered the primary epithelial polarity landmark, are required for both epithelial sheet formation and maintenance. After stage 6, the follicle cells undergo complex morphogenetic processes associated with changes in adherens junction levels (SPRADLING 1993; WU *et al.* 2008). The Drosophila β-catenin encoded by the *armadillo* (*arm*) locus is enriched at the adherens-type junctions. Arm protein is abundantly expressed in follicle cell epithelium and is enriched at the apical-lateral plasma membrane surface juxtaposed to the germline (PEIFER *et al.* 1993). To determine if EcR-B1 knockdown defects in follicular epithelium integrity were associated with altered AJ structure, we examined the localization of the Arm protein in egg chambers from females overexpressing the *EcR-B1* RNAi transgene under the control of the *Cy2-Gal4* driver (Figure 3, D–F′). Arm staining was also performed on egg chambers from control females overexpressing the *UAS-GFP* transgene under the control of the same *Cy2-Gal4* driver (Figure 3, A and C). Compared with staining of control egg chambers, we observed two significant changes in Arm accumulation: (1) in cells that remain in contact with the germline, Arm accumulation is either strong (see arrow in Figure 3, D′ and F′) or barely detectable (see arrowhead in Figure 3, D′ and F′) and (2) in follicle cells that delaminate from the follicular epithelium, apical Arm staining is quite absent (see asterisks in Figure 3, D′ and F′). Multilayering of follicle cells was also observed in egg chambers expressing the *UAS-IR-EcR-B1* transgene under the control of the *E4-Gal4* driver (Figure 3, H and H′) that drives Gal4 expression starting from stage 7 (QUEENAN *et al.* 1997) (supplemental Figure 1) and in these egg chambers, the same alterations of Arm protein distribution were recognized (Figure 3, G, G′, I, and I′). Detection of the same phenotypic response with different Gal4 drivers (in Figure 3 compare D–F′ to G–I′) provides strong evidence that EcR-B1 is required

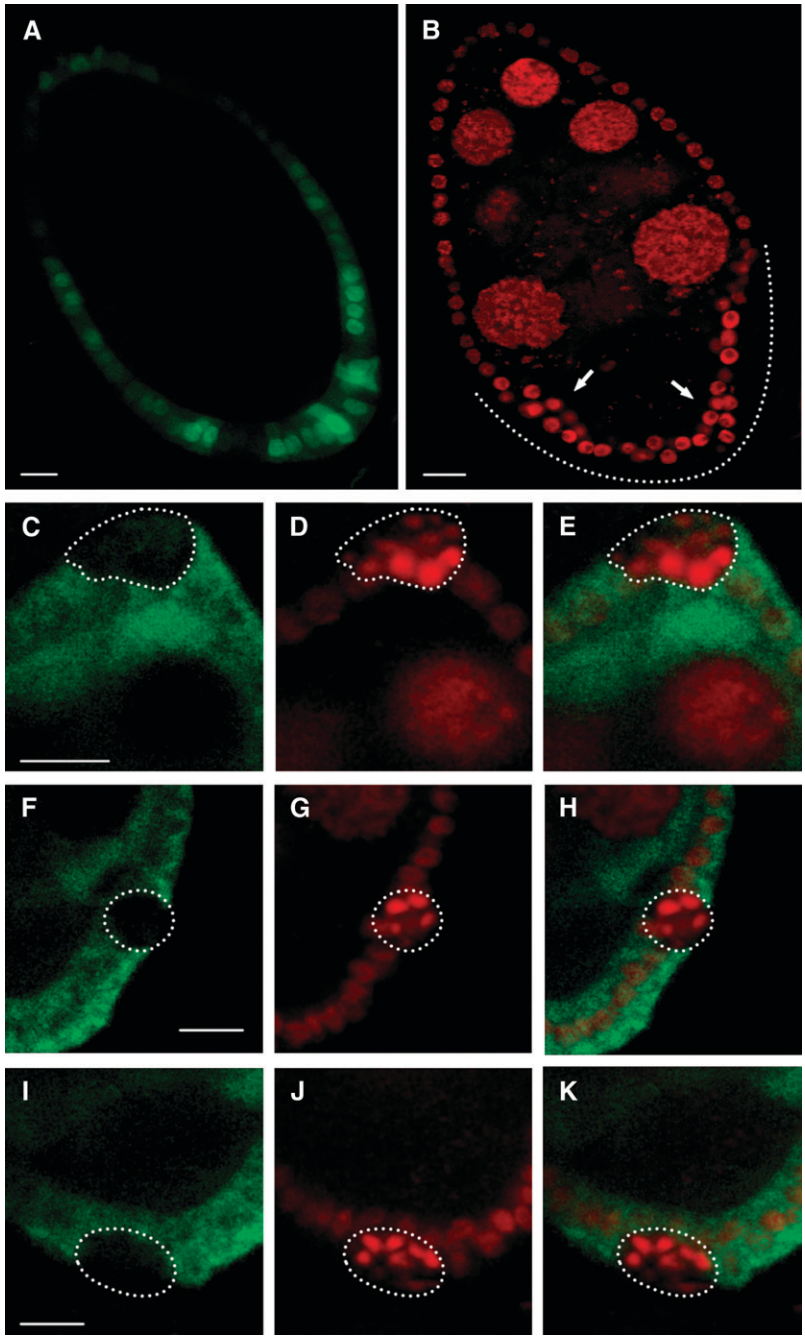

FIGURE 2.—Silencing of *EcR-B1* in follicle cells at midoogenesis disrupts follicular epithelium integrity. Confocal cross-sections of stage 8 egg chambers from females expressing the *UAS-GFP* reporter (A; green) or the *UAS-IR-EcR-B1* transgene (B–K) under the control of the *Cy2-Gal4* driver. Propidium iodide staining allows the detection of multilayered follicle cells (dotted line in B and dotted areas in D, G, and J). EcR-B1 protein (C, F, and I; green) is undetectable in multilayered follicle cells localized in anterior (E), lateral (H), and posterior (K) areas of the follicular epithelium. Bars, 10 μm.

in follicle cells to maintain proper architecture of the follicular epithelium.

We next analyzed the localization of AJ core proteins to investigate if EcR-B1 knockdown in follicle cells affects their distribution. AJs are complexes composed of cadherin transmembrane proteins linked to cytoplasmic β-catenin, α-catenin, and actin (TEPASS *et al.* 2001; MÜLLER and BOSSINGER 2003). The extracellular domain of DE-cadherin (DE-Cad) mediates cell–cell adhesion while the highly conserved intracellular domain is linked to the actin cytoskeleton via a carboxyl-terminal domain that binds to a β-catenin/α-catenin complex to link to the actin cytoskeleton (KNUST 2002; HALBLEIB and NELSON 2006). To investigate AJ structure in egg chambers from *Cy2-Gal4; UAS-IR-EcR-B1* females we analyzed the localization of DE-Cad and the F-actin cytoskeleton. DE-Cad levels are strongly reduced (Figure 4, A–C′) in multilayered follicle cells (see arrows in Figure 4, A′ and C′) and similar to Arm localization, the F-actin cytoskeleton is not detectable in delaminating follicle cells (Figure 4, D–F′; see bracket in Figure 4, D′–F′).

We next analyzed the effect of *EcR-B1* silencing on the basolateral junction (BLJ) that interconnects follicle cells and that contains proteins conserved in vertebrate epithelia. We focused on two proteins in particular, Dlg and Scrib, which are localized to lateral domains of the

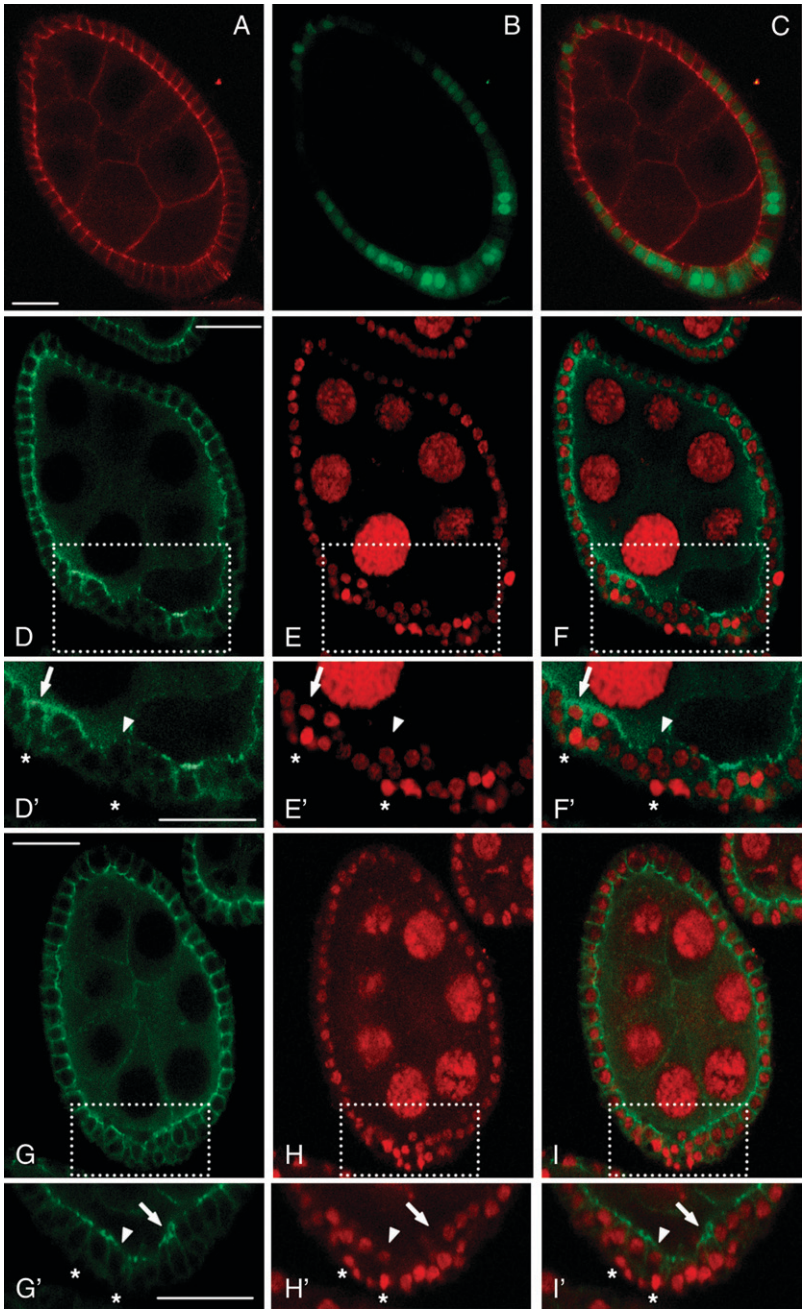

Figure 3.—Knockdown of EcR-B1 isoform in follicle cells at midoogenesis affects AJ core components. Confocal cross-sections of a stage 8 egg chamber from females expressing the *UAS-GFP* reporter (B; green) under the control of the *Cy2-Gal4* driver. The *Gal4*-induced GFP expression is uneven due to the *Cy2-Gal4* driver activity. Arm protein (A; red) is abundantly expressed in the follicular epithelium and is enriched at the apical and lateral surfaces of the plasma membranes that are juxtaposed to the germline cells. Merged image of GFP and Arm signals is shown in C. Confocal cross-sections of stage 8 egg chambers from females overexpressing the *UAS-IR-EcR-B1* transgene under the control of the *Cy2-Gal4* driver (D–F′) or the *E4-Gal4* driver (G–I′). D′–I′ are higher magnification views of the boxed regions in D–I, respectively. Knockdown of EcR-B1 causes multilayering of follicle cells, as assessed by propidium iodide staining (E, E′, H, and H′; red) and altered localization of Arm protein (D, D′, G, and G′; green). F, F′, I, and I′ are merged images of Arm (D, D′, G, and G′) and propidium iodide (E, E′, H, and H′) stainings. Follicle cells facing the germline show either strong (see arrows in D′, F′, G′, and I′) or quite absent (see arrowheads in D′, F′, G′, and I′) Arm staining. In the misplaced follicle cells, Arm staining is undetectable (see asterisks in D′, F′, G′, and I′). Anterior is up in all panels. Bars, 20 μm.

cell membrane, just basal to the AJs to form a barrier known as septate junction, and are analogous to the tight junction of mammalian cells (Knust 2002). Immunodetection of the Dlg protein in egg chambers expressing the *UAS-IR-EcR-B1* transgene under the *Cy2-Gal4* driver showed an aberrant circumferential localization of this protein in delaminating follicle cells (Figure 5, A–C′, see asterisks in A′–C′). Multilayered follicle cells also showed aberrant distribution of the Scrib protein that is present in both apical and lateral domains (Figure 5, D–F′, see asterisk in D′–F′). In addition, *UAS-IR-EcR-B1* follicle cells whose nuclei show high levels of DNA staining also exhibit aberrant basal localization of the Scrib protein (see arrowheads in Figure 5, D′–F′). We then investigated the localization of aPKC, a functionally conserved component of an apical protein complex that includes Par6 and Baz (Müller and Bossinger 2003) and regulates apical-basal polarity in both epithelial and nonepithelial cell types. In wild-type follicle cells, aPKC localizes to the apical membrane (Cox *et al.* 2001); however, knockdown of the EcR-B1 isoform causes a reduction of aPKC levels in follicle cells facing the germline and undetectable levels in delaminating follicle cells (see bracket in Figure 5, G′–I′), consistent with defective polarity in cells with reduced EcR-B1 activity (Figure 5, G–I′, see arrowheads in Figure 5, G′–I′). In summary these data show that reduced EcR-B1 level is associated with the loss of apico-basal polarity in follicle

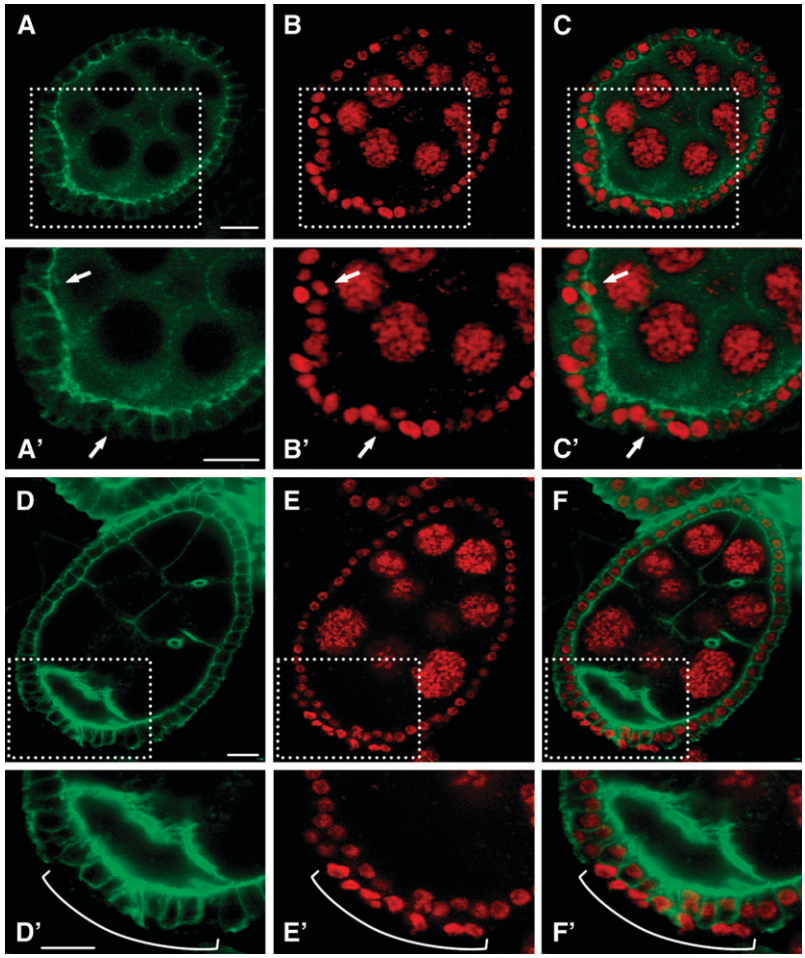

FIGURE 4.—Silencing of *EcR-B1* in follicle cells at midoogenesis disrupts apico-basal polarity. Confocal cross-sections of stage 7 (A–C′) and stage 8 (D–F′) egg chambers from females overexpressing the *UAS-IR-EcR-B1* transgene under the control of the *Cy2-Gal4* driver. A′–F′ are higher magnification views of the boxed region in A–F, respectively. Knockdown of EcR-B1 causes multilayering of follicle cells, as assessed by propidium iodide staining (B, B′, E, and E′; red). These misplaced follicle cells exhibit loss of apical polarity, as assessed by alteration of DE-Cad distribution (A and A′; green) and loss of F-actin cytoskeleton (D and D′; green). C, C′, F, and F′ are merged images of propidium iodide (B, B′, E, and E′), DE-Cad (A and A′) and FITC-phalloidin (D and D′) stainings. DE-Cad staining is lowered in multilayered follicle cells (arrows in A′). F-actin staining is not detectable in delaminating follicle cells (bracket in D′–F′). Anterior is up in all panels. Bars, 10 μm.

cells. Because delamination of follicle cells can arise from activation of an apoptotic cell death program, we used the TUNEL technique to detect DNA fragmentation resulting from programmed cell death (GAVRIELI *et al.* 1992) in *Cy2-Gal4; UAS-IR-EcR-B1* females. As shown in supplemental Figure 2, no TUNEL staining was detectable in multilayered follicle cells of egg chambers in which EcR-B1 levels were reduced after stage 7.

EcR-B1 depletion in clones of follicle cells affects follicular epithelium integrity and follicle cell survival: Tissue- and stage-specific knockdown of EcR-B1 isoform determined its role in maintaining proper follicle cell polarity and follicular epithelium integrity at midoogenesis. We performed next a clonal analysis of EcR-B1 receptor to knock down its function also at earlier stages of oogenesis. Using the Flp-out/Gal4 technique (PIGNONI and ZIPURSKY 1997), we randomly expressed the *UAS-IR-EcR-B1* transgene under the actin promoter in clonal patches of cells by using the Flp-out cassette driver *Act5C>CD2>Gal4* and a *heat-shock-Flp-recombinase* (*hs-Flp*). Clones were produced prior to stage 6 and the locations of knockdown clones were mapped by the absence of the membrane-targeted CD2 marker. Extensive analyses of these egg chambers revealed that EcR-B1 silencing in follicle cell clones at early stages also resulted in multilayering and loss of proper columnar monolayer organization, similar to knockdown at later stages (data not shown). In addition, in follicle cell clones expressing the *UAS-IR-EcR-B1*, marked by the absence of the CD2 marker (Figure 6, A and A′), many picnotic nuclei are detected (Figure 6, B, B′, C, and C′). Immunostaining of these egg chambers with anti-EcR-B1 antibody confirmed that clonal expression of the RNA interfering transgene was effective in reducing EcR-B1 levels (Figure 6D). Follicle cell picnotic nuclei (Figure 6E) were always detectable in follicular epithelium areas of strongly decreased EcR-B1 levels (see dotted areas in Figure 6, D and E). Strongly reduced size of follicle cell nuclei could arise from an extension of the proper proliferative program beyond stage 6 and consequent reduced endocycling of follicle cells. By using the PH3 antibody previously described, we did not find any PH3-positive cells after stage 6 (data not shown). TUNEL positivity was detected in *UAS-IR-EcR-B1* follicle cell clones (Figure 6H) that exhibited as well a condensed state of chromatin as judged by DAPI staining (Figure 6, F and G). These data indicate that cells with reduced EcR-B1 levels undergo apoptosis. We next analyzed these egg chambers with active caspase-3 antibody (PETERSON *et al.* 2003). Caspase activity (Figure 7,

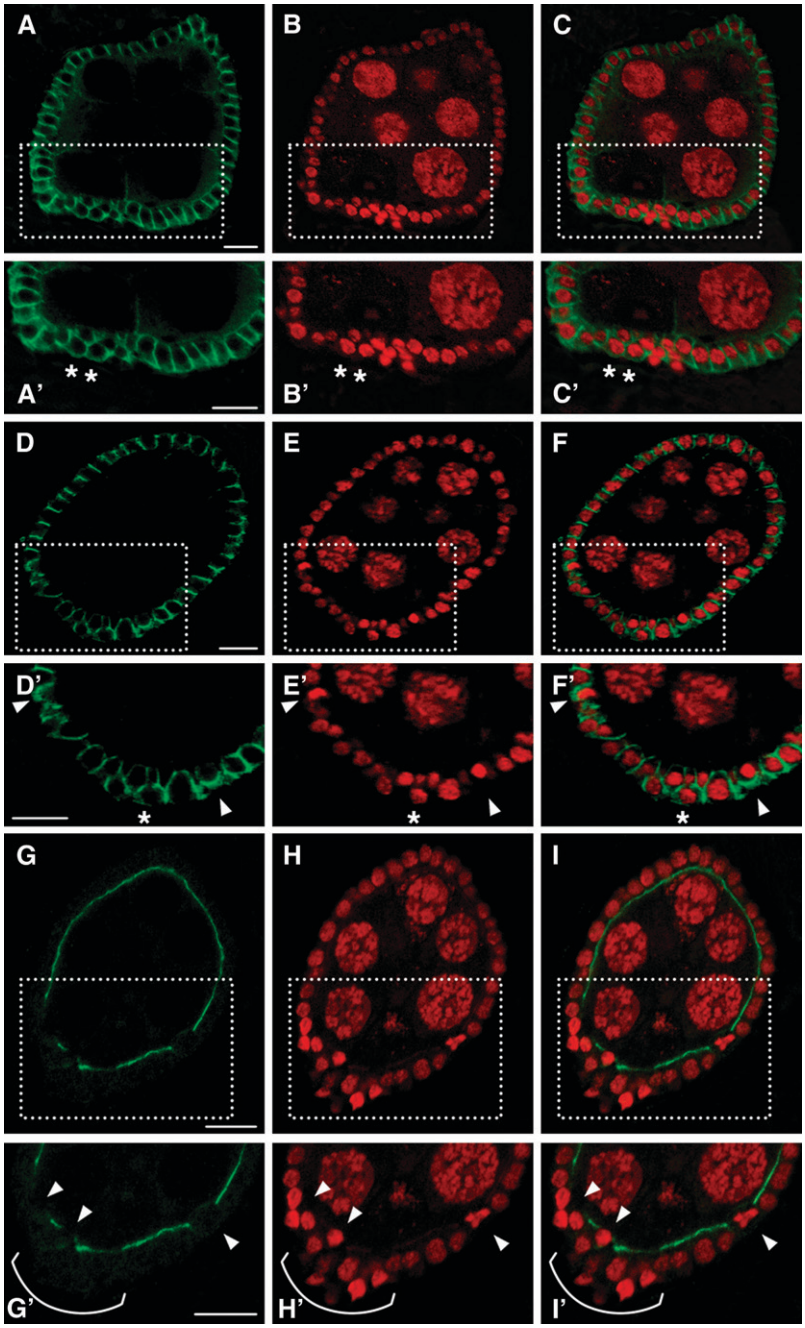

FIGURE 5.—Knockdown of EcR-B1 isoform in follicle cells affects apical and basolateral polarity. Confocal cross-section of stage 7 egg chambers from females in which the *Cy2-Gal4* driver controls the *UAS-IR-EcR-B1* expression (A–I′). Boxed areas in A–I are enlarged in A′–I′, respectively. Propidium iodide staining shows the piling up of follicle cells whose nuclei are strongly stained and show altered shape (B, B′, E, E′, H, and H′; red). Dlg immunodetection (A and A′; green) in multilayered follicle cells (asterisks in A′–C′) shows a circumferential localization of this protein (C′; merged propidium iodide and Dlg signals). The Scrib signal (D and D′; green) is detected at higher levels and it is mislocalized. Follicle cells with strong nuclei staining show a basal Scrib localization (see arrowheads in D′, E′, and in their merge F′). Asterisks in D′–F′ point to a delaminating follicle cell that exhibit apico-lateral distribution of the Scrib signal. Apical aPKC localization (G and G′; green) in multilayered follicle cells (H and H′; red) is absent (I and I′; merged propidium iodide and aPKC signals) (see bracket in G′–I′). Also some follicle cells facing the germline lack apical aPKC staining (see arrowheads in G′–I′). Anterior is up in all panels. Bars, 10 μm.

B and B′) was detected in follicle cell clones overexpressing the *EcR-B1* interfering transgene (Figure 7, C, C′, D, and D′). Interestingly, caspase-3 immunoreactivity is detected in these follicle cell clones exhibiting highly condensed nuclei (Figure 7, A, A′, D, and D′).

We then analyzed the Drosophila inhibitor of apoptosis protein 1 (Diap1) a potent caspase inhibitor that is essential to prevent inappropriate caspase activation and ubiquitous apoptosis (WANG *et al.* 1999; GOYAL *et al.* 2000). This antiapoptotic protein is ubiquitously expressed at stage 9 and 10 of oogenesis in follicle cells (GEISBRECHT and MONTELL 2004). Diap1 is involved in PCD that occurs at the mid-oogenesis checkpoint and that leads to egg chambers degeneration in response to poor environmental conditions. It has been reported that degenerating egg chambers exhibit strongly lowered levels of Diap1 cytoplasmic staining in nurse cells while high levels of caspase-3 activity is detectable throughout the egg chambers (BAUM *et al.* 2007). Co-immunostaining of egg chambers clonally expressing the *UAS-IR-EcR-B1* transgene showed a dramatic downregulation of Diap1 (Figure 7, F and F′) that is concomitant with high levels of caspase-3 activity (Figure 7, G and G′) in follicle cells exhibiting highly condensed nuclei (Figure 7, E, E′, H, and H′). These results indicate that knocking down the EcR-B1 isoform at early stages of oogenesis alters both proper follicular epithelium monolayer structure and leads to premature apoptotic follicle cell death.

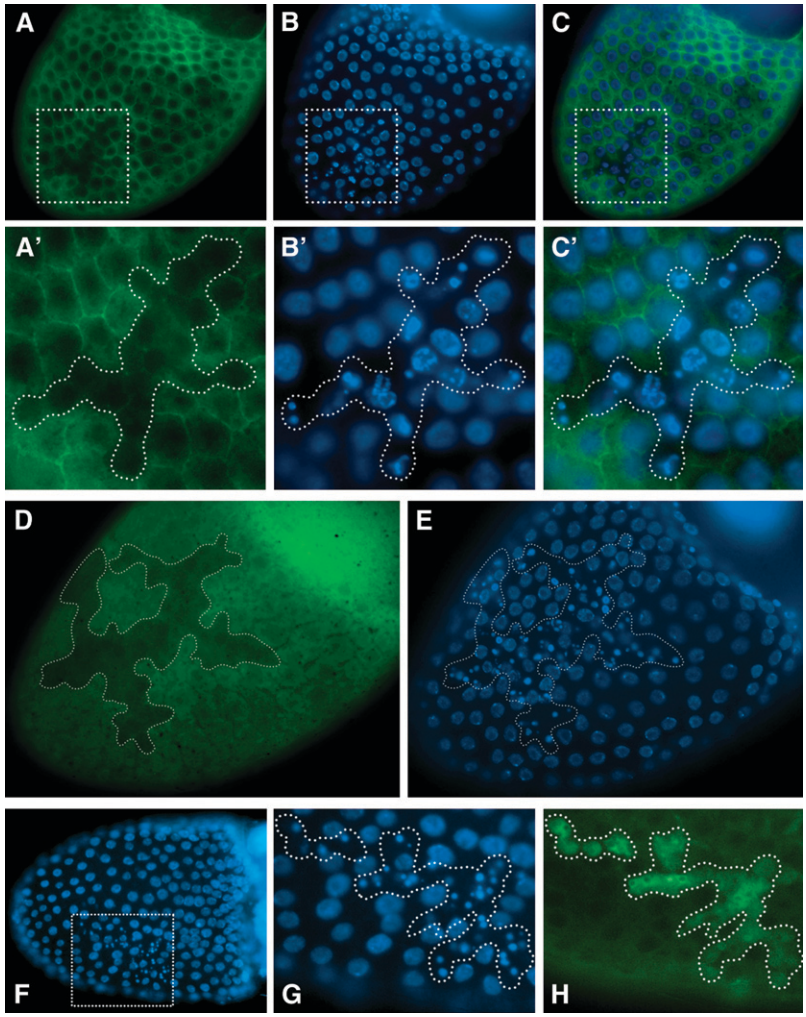

Figure 6.—Clonal knockdown of EcR-B1 results in multilayering and apoptotic death of follicle cells. Fluorescence images (A–C′) of a stage 10B egg chamber from females overexpressing the *UAS-IR-EcR-B1* silencing transgene in clonal patches of follicle cells marked by the absence of the CD2 marker (A and A′; green). Picnotic nuclei are detected by DAPI staining (B and B′; blue) in follicle cell clones overexpressing the RNAi transgene (C and C′; merged CD2 and DAPI signals). A′–C′ are higher magnification views of the boxed areas in A–C. Fluorescence images (D and E) of a stage 10B egg chamber from females of the same genotype. Anti-EcR-B1 staining (D; green) shows decreased Ecr-B1 protein level in a large area of the follicular epithelium (dotted area in D) containing many picnotic nuclei (DAPI staining, E; blue) Fluorescence images (F–H) of a stage 10B egg chamber from females of the same genotype. Picnotic nuclei (dotted area in G), detected by DAPI staining (F and G; blue), exhibit TUNEL positivity (dotted area in H; green). G and H are higher magnification views of the boxed area in F. Posterior is toward the left in all panels.

DISCUSSION

In Drosophila, proper oogenesis results from a number of developmental decisions that require ecdysone, ecdysone receptor (EcR), and ecdysone response genes (Riddiford *et al.* 2000). Our functional analysis shows that the EcR-B1 isoform plays a key role in follicular epithelium maintenance throughout oogenesis.

EcR-B1 and follicle cell polarity: Tissue-specific silencing of *EcR-B1* at early and mid-stages of oogenesis results in delamination of follicle cells and loss of follicular monolayer integrity. The analysis of different cell polarity markers shows that targeting *EcR-B1* interference at stage 7 of oogenesis causes the complete loss of follicle cell polarity. The AJ components DE-Cad and Arm fail to localize apically and the F-actin cytoskeleton is strongly affected in multilayered follicle cells. Cadherin-mediated adhesive junctions play a major role in epithelial polarization and are integral to the proper assembly of the lateral surface domain. Accordingly, our analysis of distribution of Dlg and Scrib components of the BLJ shows that basolateral polarity is altered in follicle cells in which the EcR-B1 function was silenced. Finally, the apical marker aPKC failed to localize to the cortex indicating a loss of apical membrane identity. We found that multilayering of follicle cells is not due to loss of proliferative control. It has been shown previously that induction of follicle cell apoptosis by expression of the *reaper* gene causes a decline of Arm levels that is coincident with nuclear condensation (Chao and Nagoshi 1999). Our results show that quite undetectable Arm levels are observed in EcR-B1 knockdown follicle cells whose nuclei do not exhibit any sign of condensation, suggesting that decrease of Arm signal does not arise from proteolytic cleavage driven by apoptotic machinery. In support of this, *EcR-B1* mutant cells are negative to TUNEL assay. We conclude that the reported abnormalities of polarity markers following late knockdown of EcR-B1 do not arise from cytological events associated with apoptosis. The ecdysone pathway is involved in the control of turnover of cadherin-containing cell adhesion complexes in border cells. It has been reported that loss of *usp* function in border cells results in a block to their migration and that Taiman, coactivator of the EcR/USP receptor complex, stimulates turnover of adhesion complexes to allow forward movement of border cells

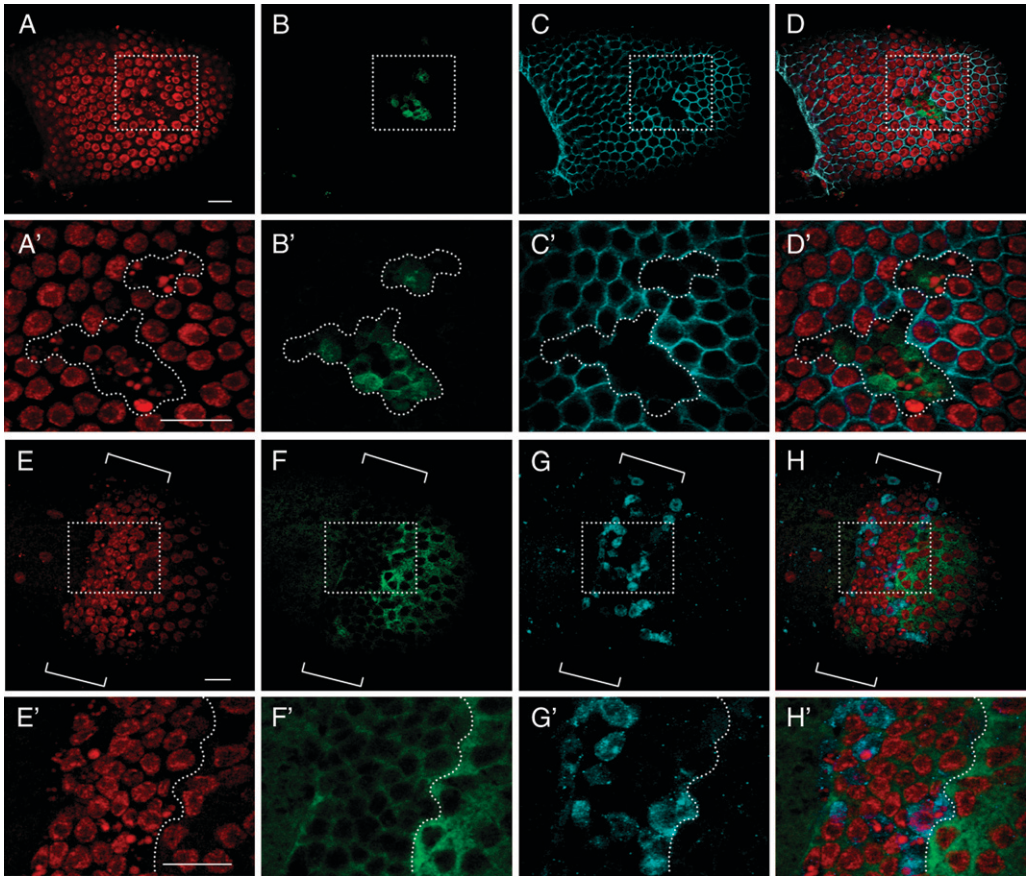

FIGURE 7.—Silencing of *EcR-B1* in clones of follicle cells causes caspase-3 activation and Diap1 downregulation. Confocal images of stage 10B mosaic egg chambers expressing the *UAS-IR-EcR-B1* transgene (A–H′). Double immunolabeling with anti-active caspase-3 (B and B′; green) and anti-CD2 (C and C′; cyan) coupled with propidium iodide staining (A and A′; red) shows that in clones expressing the *EcR-B1* interfering transgene, follicle cells with highly condensed nuclei and active caspase-3 are recognizable (D and D′; merge of all signals). Egg chamber from females of the same genotype immunostained with anti-Diap1 (F and F′; green), anti-cleaved caspase-3 (G and G′; cyan) and stained with propidium iodide (E and E′; red). H and H′ are merged images of all signals. The brackets in E–H point to a wide area of strongly decreased Diap1 staining in follicular epithelium (F). In this area, follicle cells showing highly condensed nuclei (E) and active caspase-3 (G) are detectable. Higher magnification views of the boxed areas in E–H are shown in E′–H′ where a dotted line marks the border between very low levels (left) and high levels (right) of Diap1 staining. Anterior is left in all panels. Bars, 20 μm.

(BAI *et al.* 2000). Thus it is possible to hypothesize that the EcR-B1-mediated ecdysone signaling controls the turnover of AJ components in the follicle cells surrounding the egg chamber.

EcR-B1 and follicle cell death: Our clonal analysis shows that targeted RNA interference of *EcR-B1* at early stages of oogenesis, when follicle cells are still actively proliferating, induces apoptotic follicle cell death beside loss of monolayer integrity. The EcR-B1 isoform is required in a cell-autonomous manner, since mutant phenotypes do not extend to the surrounding wild-type tissue. We found that targeted knockdown of EcR-B1 function causes a strong Diap1 downregulation. Diap1 constitutes a central point of control during apoptosis and females carrying a combination of two viable alleles of *diap1* exhibit ovarian degeneration (XU *et al.* 2005). During oogenesis, two developmental checkpoints monitor the egg chamber to allow the development of healthy oocyte or the death of defective egg chambers by apoptosis. These checkpoints act in the region 2A of the germarium and at stages 8–9 during midoogenesis, respectively (MCCALL 2004). The ecdysone pathway is involved in the developmental checkpoint at stage 8 of oogenesis and in the apoptotic death of nurse cells occurring during nutritional shortage at stages 8 and 9 of oogenesis. It has been shown that starvation leads to a rapid increase of ecdysteroid levels in the ovaries and that this high concentration results in apoptotic cell death of nurse cells (BOWNES 1989; TERASHIMA and BOWNES 2004; TERASHIMA *et al.* 2005). Interestingly, it has been reported that Diap1 expression in nurse cells is downregulated at stages 7–8 when midoogenesis checkpoint acts, and again at stage 11 when developmentally PCD occurs (BAUM *et al.* 2007). In addition, degenerating midoogenesis egg chambers exhibit low levels of Diap1 in nurse cells that are coincident with intense activity of caspase-3. Of interest, in EcR-B1 knockdown follicle clones we detected downregulation of Diap1 and activation of caspase-3. Moreover these follicle cells exhibit strong nuclear condensation and DNA fragmentation witnessed by TUNEL positivity. It is then possible to hypothesize that in the follicle cells the EcR regulates the same molecular machinery acting in nurse cells to execute PCD. Alternatively, the apoptotic phenotype that arises from *EcR-B1* silencing at early stages of oogenesis could be a more indirect effect of reduced ecdysone signaling. Loss of EcR-B1 function at early stages of oogenesis causes piling up of follicle cells. The presence of delaminating follicle cell stretches in early-stage egg chambers

could represent a defect that is recognized by the midoogenesis checkpoint. This checkpoint could then trigger apoptosis to eliminate these defective egg chambers. Since the midoogenesis checkpoint acts at stages 7–8, silencing of the *EcR-B1* at later stages results in multilayered phenotype without follicle cell death.

We thank Trudi Schüpbach for the generous gifts of Drosophila strains that were essential for this study. We also thank the Bloomington Stock Center for providing us with fly stocks. We are particularly grateful to the Developmental Studies Hybridoma Bank at the University of Iowa for antibodies. We also thank C. Doe and B. Hay for gifting us the anti-Scribble and anti-Diap1 antibodies. We thank Marco Privitera for his skillful graphic work. We also thank two anonymous reviewers and the editor for helpful comments on the manuscript. This work was supported by a research grant from the Ministero dell'Università e della Ricerca and from the University of Bologna (Prin 2006/2008), and a research grant from University of Bologna (RFO 2006) to G.G. and V.C., and fellowships from the University of Bologna (to P.R. and F.B.). This work was also supported by a research grant from the National Science Foundation (RPG-00251-01-DDC), and a University of Missouri-Kansas City Faculty Research grant to L.L.D. and a Chancellor's graduate fellowship (to J.F.H.).

LITERATURE CITED

Andrenacci, D., F. M. Cernilogar, C. Taddei, D. Rotoli, V. Cavaliere *et al.*, 2001 Specific domains drive VM32E protein distribution and integration in *Drosophila* eggshell layers. J. Cell Sci. **114:** 2819–2829.

Bai, J., Y. Uehara and D. J. Montell, 2000 Regulation of invasive cell behavior by Taiman, a *Drosophila* protein related to AIB1, a steroid receptor coactivator amplified in breast cancer. Cell **103:** 1047–1058.

Baum, J. S., E. Arama, H. Steller and K. McCall, 2007 The *Drosophila* caspases Strica and Dronc function redundantly in programmed cell death during oogenesis. Cell Death Differ. **14:** 1508–1517.

Bownes, M., 1989 The roles of juvenile hormone, ecdysone and the ovary in the control of *Drosophila* vitellogenesis. J. Insect Physiol. **34:** 409–413.

Brand, A. H., and N. Perrimon, 1993 Targeted gene expression as a means of altering cell fates and generating dominant phenotypes. Development **118:** 401–415.

Carney, G. E., and M. Bender, 2000 The *Drosophila* ecdysone receptor (EcR) gene is required maternally for normal oogenesis. Genetics **154:** 1203–1211.

Cavaliere, V., C. Taddei and G. Gargiulo, 1998 Apoptosis of nurse cells at the late stages of oogenesis of *Drosophila melanogaster*. Dev. Genes Evol. **208:** 106–112.

Chao, S., and R. N. Nagoshi, 1999 Induction of apoptosis in the germline and follicle layer of *Drosophila* egg chambers. Mech. Dev. **88:** 159–172.

Cox, D. N., S. Abdelilah-Seyfried, L. Y. Jan and Y. N. Jan, 2001 Bazooka and atypical protein kinase C are required to regulate oocyte differentiation in the *Drosophila* ovary. Proc. Natl. Acad. Sci. USA **98:** 14475–14480.

Danial, N. N., and S. J. Korsmeyer, 2004 Cell death: critical control points. Cell **116:** 205–219.

Deng, W. M., C. Althauser and H. Ruohola-Baker, 2001 Notch-Delta signaling induces a transition from mitotic cell cycle to endocycle in *Drosophila* follicle cells. Development **128:** 4737–4746.

Gavrieli, Y., Y. Sherman and S. A. Ben-Sasson, 1992 Identification of programmed cell death in situ via specific labeling of nuclear DNA fragmentation. J. Cell Biol. **119:** 493–501.

Geisbrecht, E. R., and D. J. Montell, 2004 A role for *Drosophila* IAP1-mediated caspase inhibition in Rac-dependent cell migration. Cell **118:** 111–125.

Goyal, L., K. McCall, J. Agapite, E. Hartwieg and H. Steller, 2000 Induction of apoptosis by *Drosophila reaper*, *hid* and *grim* through inhibition of IAP function. EMBO J. **19:** 589–597.

Hackney, J. F., C. Pucci, E. Naes and L. Dobens, 2007 Ras signaling modulates activity of the ecdysone receptor EcR during cell migration in the *Drosophila* ovary. Dev. Dyn. **236:** 1213–1226.

Halbleib, J. M., and J. Nelson, 2006 Cadherins in development: cell adhesion, sorting and tissue morphogenesis. Genes Dev. **20:** 3199–3214.

Kennerdell, J. R., and R. W. Carthew, 2000 Heritable gene silencing in *Drosophila* using double-stranded RNA. Nat. Biotechnol. **18:** 896–898.

Knust, E., 2002 Regulation of epithelial cell shape and polarity by cell-cell adhesion. Mol. Membr. Biol. **19:** 113–120.

Koelle, M. R., W. S. Talbot, W. A. Segraves, M. T. Bender, P. Cherbas *et al.*, 1991 The *Drosophila EcR* gene encodes an ecdysone receptor, a new member of the steroid receptor superfamily. Cell **67:** 59–77.

McCall, K., 2004 Eggs over easy: cell death in the *Drosophila* ovary. Dev. Biol. **274:** 3–14.

McGuire, S. E., P. T. Le, A. J. Osborn, K. Matsumoto and R. L. Davis, 2003 Spatiotemporal rescue of memory dysfunction in *Drosophila*. Science **302:** 1765–1768.

Müller, H. A., and O. Bossinger, 2003 Molecular networks controlling epithelial cell polarity in development. Mech. Dev. **120:** 1231–1256.

Peifer, M., S. Orsulic, D. Sweeton and E. Wieschaus, 1993 A role for the *Drosophila* segment polarity gene *armadillo* in cell adhesion and cytoskeletal integrity during oogenesis. Development **118:** 1191–1207.

Peterson, J. S., M. Barkett and K. McCall, 2003 Stage-specific regulation of caspase activity in *Drosophila* oogenesis. Dev. Biol. **260:** 113–123.

Pignoni, F., and S. L. Zipursky, 1997 Induction of *Drosophila* eye development by Decapentaplegic. Development **124:** 271–278.

Queenan, A. M., A. Ghabrial and T. Schüpbach, 1997 Ectopic activation of *torpedo/Egfr*, a *Drosophila* receptor tyrosine kinase, dorsalizes both the eggshell and the embryo. Development **124:** 3871–3880.

Riddiford, L. M., P. Cherbas and J. W. Truman, 2000 Ecdysone receptors and their biological actions. Vitam. Horm. **60:** 1–73.

Roignant, J. Y., C. Carrè, B. Mugat, D. Szymczak, J. A. Lepesant *et al.*, 2003 Absence of transitive and systemic pathways allows cell-specific and isoform-specific RNAi in *Drosophila*. RNA **9:** 299–308.

Spradling, A. C., 1993 Developmental genetics of oogenesis, pp. 1–70 in *The Development of Drosophila melanogaster*, edited by M. Bate and A. Martinez-Arias. Cold Spring Harbor Laboratory Press, Cold Spring Harbor, NY.

Steller, H., 2008 Regulation of apoptosis in *Drosophila*. Cell Death Differ. **15:** 1132–1138.

Talbot, W. S., E. A. Swyryd and D. S. Hogness, 1993 *Drosophila* tissues with different metamorphic responses to ecdysone express different ecdysone receptor isoforms. Cell **73:** 1323–1337.

Tepass, U., G. Tanentzapf, R. Ward and R. Fehon, 2001 Epithelial cell polarity and cell junctions in *Drosophila*. Annu. Rev. Genet. **35:** 747–784.

Terashima, J., and M. Bownes, 2004 Translating available food into the number of eggs laid by *Drosophila melanogaster*. Genetics **167:** 1711–1719.

Terashima, J., and M. Bownes, 2005 A microarray analysis of genes involved in relating egg production to nutritional intake in *Drosophila melanogaster*. Cell Death Differ. **12:** 429–440.

Terashima, J., K. Takaki, S. Sakurai and M. Bownes, 2005 Nutritional status affects 20-hydroxyecdysone concentration and progression of oogenesis in *Drosophila melanogaster*. J. Endocrinol. **187:** 69–79.

Wang, S. L., C. J. Hawkins, S. J. Yoo, H. A. Muller and B. A. Hay, 1999 The *Drosophila* caspase inhibitor DIAP1 is essential for cell survival and is negatively regulated by HID. Cell **98:** 453–463.

Wu, X., P. S. Tanwar and L. A. Raftery, 2008 *Drosophila* follicle cells: morphogenesis in an eggshell. Semin. Cell Dev. Biol. **19:** 271–282.

Xu, D., Y. Li, M. Arcaro, M. Lackey and A. Bergmann, 2005 The CARD-carrying caspase Dronc is essential for most, but not all, developmental cell death in *Drosophila*. Development **132:** 2125–2134.

Yin, V. P., and C. S. Thummel, 2005 Mechanisms of steroid-triggered programmed cell death in *Drosophila*. Semin. Cell Dev. Biol. **16:** 237–243.

Communicating editor: T. Schüpbach